Mathematical Biosciences and Engineering

https://www.aimspress.com/journal/mbe

MBE, 22(12): 3088–3106.
DOI: 10.3934/mbe.2025114
Received: 16 June 2025
Revised: 27 August 2025
Accepted: 04 September 2025
Published: 17 October 2025

Research article

A compartmental epidemic model with age stratification for insurance premium calculation

Shirali Kadyrov[1,2], Gauhar Kayumova[1], Asilbek Yallaboyev[1] and Bizhigit Sagidolla[2,*]

[1] New Uzbekistan University, Tashkent 100000, Uzbekistan
[2] SDU University, Kaskelen 040900, Kazakhstan

* **Correspondence:** Email: bizhigit.sagidolla@sdu.edu.kz.

Abstract: This paper develops a mathematical framework for life and health insurance premium calculation under epidemic conditions, incorporating age-structured population dynamics and disease compartments. We proposed a compartmental epidemic model with three age groups and four states (susceptible, infectious, recovered, deceased) to reflect heterogeneity in disease progression and risk exposure. The model captures differential mortality and morbidity risks across age groups and infection states, enabling dynamic adjustment of insurance premiums. By integrating actuarial principles with epidemic-driven transition probabilities, we derived explicit premium formulas and validated them through numerical simulations. Our results demonstrate that age stratification and detailed infection stages significantly impact premium pricing, particularly for older populations with higher mortality risks. Sensitivity analysis reveals that recovery and mortality rates are key drivers of premium variability. The framework provides insurers with a robust tool for pandemic risk assessment, ensuring solvency while maintaining affordability.

Keywords: epidemic modeling; age stratification; health insurance; premium calculation; actuarial principles; SIRD model; hospitalization costs; parameter estimation; sensitivity analysis; disease dynamics; genetic algorithm

1. Introduction

The COVID-19 pandemic has underscored the need for adaptive insurance frameworks to address dynamic health risks. Recent studies emphasize integrating epidemiological models with actuarial principles to price insurance products during epidemics. Francis et al. [1–3] extended multi-state Markov models to include contagion effects, enabling individual risk assessment. Zhai et al. [4] proposed a susceptible-exposed-infected-containing-3-substates-recovered-dead model, calibrated to COVID-19 data, to derive fair premiums and reserve trajectories. Arthur et al. [5] highlighted

age-specific heterogeneity in contact patterns and mortality, showing complex dynamics at lower transmissibility. These works underscore the importance of age-structured models for accurate risk classification [6, 7].

Compartmental models are foundational for epidemic forecasting. Driessche and Watmough [8] provided the mathematical basis for the basic reproduction number R_0, critical for stability analysis. Recent advances refined these models for greater granularity. For instance, Amemiya et al. [9] developed an age-dependent final size equation to estimate COVID-19 mortality in China, emphasizing the critical role of age-specific contact matrices and vaccination coverage in predicting health outcomes, which informed our age-stratified approach. Similarly, Yan and Liu [10] introduced a compartmental model with nonlinear incidence rates driven by disease-related contact functions, offering insights into dynamic transmission processes that align with our model's extended infection states. Other extensions addressed asymptomatic and dead-infective subpopulations with feedback controls, as in the SEIADR framework of Sen et al. [11], or vertical transmission with media influence as studied by Shah et al. [12], both of which highlight the importance of incorporating additional biological and behavioral factors into epidemic modeling. Furthermore, Niu et al. [13] explored the Internet of Medical Things for real-time health data integration, suggesting potential applications for enhancing epidemic models with wearable technology data to support insurance pricing. Extensions like the SVEIRD model [14] incorporate vaccination but often lack severity stratification. Zhu et al. [15] introduced spatial and relapse dynamics, while Pacheco and Lacerda [16] used Tikhonov regularization for real-time SIRD parameter estimation. Yin et al. [17] analyzed age-structured SEIRS models with time delays, identifying periodic solutions via Hopf bifurcations. Cakmakli et al. [18] enhanced SIRD models with time-varying parameters using generalized autoregressive score methods, capturing pandemic trends. In addition, bio-inspired methods such as the Ebola optimization search algorithm [19] showed how epidemic dynamics can motivate new approaches to optimization, further illustrating the broad interdisciplinary impact of epidemic modeling. Stochastic models, such as the Markov chain SIR model developed by Chaal et al. [20], predict earlier disease extinction.

In actuarial science, epidemic models inform premium and reserve calculations. Cox et al. [21] emphasized modeling financial risks under health scenarios, while Feng et al. [22] highlighted their role in public health policy. Guerra [23] applied deterministic SIR models to insurance pricing, and Harris et al. [24] noted stable life insurance premiums during COVID-19, with adjustments for high-risk groups. Ferretti et al. [25] stressed contact tracing's impact on epidemic trajectories, and Manfredi et al. [26] showed how adaptive behavior shapes transmission, both critical for insurance planning.

In this paper, we develop an age-stratified compartmental model with three age groups and four states (susceptible, infectious, recovered, and deceased), motivated by clinical variations in COVID-19 outcomes [7]. This structure captures differential risk exposure and disease progression, modeled via differential equations for dynamic premium pricing. By integrating actuarial principles with epidemic transitions, we provide a granular framework for data-informed insurance pricing during health crises. In this work, we extend the classical epidemic model by introducing age stratification into three groups, capturing heterogeneity in recovery, susceptibility, and mortality. This distinction is essential since health risks and financial burdens vary significantly across ages. By linking the age-structured model with insurance premium calculation, we show how epidemic dynamics translate into age-specific costs. The framework provides a systematic method to derive fair premiums that reflect differential risks, ensuring both insurer solvency and policyholder equity. Thus, our approach integrates epidemiological

modeling with actuarial assessment, enhancing its value for public health planning and financial risk management.

In the following sections, we formulate the age-stratified SIRD model, analyze its stability properties, and derive insurance premium calculations for term life and health insurance products. We then estimate model parameters using COVID-19 data from Uzbekistan, employing a genetic algorithm to optimize fit, and conduct a sensitivity analysis to assess the impact of key parameters on premium estimates. Finally, we discuss the implications of our findings for insurance pricing and solvency management during pandemics, highlighting limitations and future research directions.

2. Model formulation and stability analysis

We consider an age-structured compartmental epidemic model to describe the spread of an infectious disease within a population stratified into three distinct age groups, indexed by $i = 1, 2, 3$. For each age group i, individuals can occupy one of four epidemiological compartments: susceptible ($S_i(t)$), infectious ($I_i(t)$), recovered ($R_i(t)$), or deceased ($D_i(t)$). For simplicity of notation, we drop the dependence on t and simply write S_i, I_i, R_i, D_i, etc, unless we really want to emphasize the time dependence. Disease transmission occurs through contact with infectious individuals, and the progression of the disease is governed by age-specific recovery and mortality rates.

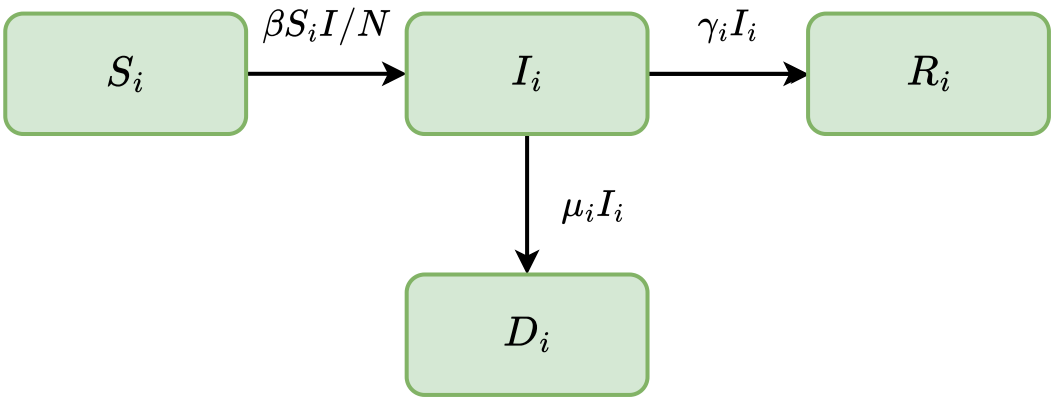

Figure 1. Age-structured SIRD model diagram with compartments S_i, I_i, R_i, and D_i.

The model dynamics, illustrated in Figure 1, are described by the following system of ordinary differential equations:

$$\begin{aligned} \frac{dS_i}{dt} &= -\frac{\beta S_i I}{N}, \\ \frac{dI_i}{dt} &= \frac{\beta S_i I}{N} - (\gamma_i + \mu_i) I_i, \\ \frac{dR_i}{dt} &= \gamma_i I_i, \\ \frac{dD_i}{dt} &= \mu_i I_i, \end{aligned} \qquad \text{for } i = 1, 2, 3, \tag{2.1}$$

where N is the initial total population, β is the transmission rate, assumed to be constant across all

age groups, and $I = \sum_{j=1}^{3} I_j$ denotes the total infectious population at time t. The parameters γ_i and μ_i represent the recovery and disease-induced mortality rates, respectively, for age group i. We assume the subpopulation in each age group satisfies:

$$N_i := S_i + I_i + R_i + D_i.$$

From (2.1), we observe that $dN_i/dt = 0$, which implies that N_i is constant. We now proceed to analyze the stability properties of this model. In particular, we will show that the susceptible population decreases over time and remains positive in the long run. Additionally, we will establish that the infected population eventually tends to zero. These results are crucial for understanding the long-term behavior of the epidemic and its eventual resolution.

Lemma 1. *Let (S_i, I_i, R_i, D_i) be a solution to the epidemic model (2.1) with initial conditions $S_i(0) > 0$, $I_i(0) \geq 0$, $R_i(0) \geq 0$, $D_i(0) \geq 0$, and where $I = \sum_j I_j$. Then the following holds:*

1) $S_i(t), I_i(t), R_i(t), D_i(t) \geq 0$ for any $t \geq 0$.
2) $S(t) := \sum_{i=1}^{3} S_i(t)$ is a non-increasing function of t, and $S(\infty) := \lim_{t\to\infty} S(t) > 0$.
3) $I(\infty) = \lim_{t\to\infty} I(t) = 0$.

Proof. **Part 1: Non-negativity of $S_i(t), I_i(t), R_i(t), D_i(t)$.** From

$$\frac{dS_i}{dt} = -\frac{\beta}{N} S_i I,$$

if $S_i(t_0) = 0$ at some t_0, then $\frac{dS_i}{dt}(t_0) = 0$, so $S_i(t) = 0$ for all $t \geq t_0$. By the uniqueness of solutions, this occurs only if $S_i(0) = 0$. Since $S_i(0) > 0$, continuity ensures $S_i(t) > 0$ for all $t \geq 0$.

For $I_i(t)$, suppose there exists $t > 0$ such that $I_i(t) < 0$. Without loss of generality, we may assume that this happens for the first time for I_1. Now, let $t_0 > 0$ be the time moment such that $I_i(t) \geq 0$ for all i and $t < t_0$, but $I_1(t_0) = 0$ and $I_1(t) < 0$ for $t > t_0$ close to t_0. At t_0,

$$\frac{dI_1}{dt}(t_0) = \frac{\beta}{N} S_1(t_0) I(t_0) \geq 0,$$

since $S_1(t_0) > 0$ and $I(t_0) = \sum I_j(t_0) \geq 0$ (as $I_j(t_0) \geq 0$ for $\forall j$). So, $I_1(t)$ cannot decrease below zero for $t > t_0$ close to t. This contradicts $I_1(t) < 0$, so $I_i(t) \geq 0$ for all $t \geq 0$.

Since $\frac{dR_i}{dt} = \gamma_i I_i \geq 0$ and $\frac{dD_i}{dt} = \mu_i I_i \geq 0$, with $R_i(0) \geq 0$ and $D_i(0) \geq 0$, it follows that $R_i(t) \geq 0$ and $D_i(t) \geq 0$ for all $t \geq 0$.

Part 2: $S(t)$ is non-increasing and $S(\infty) > 0$. Since $\frac{\beta S_i I}{N} \geq 0$,

$$\frac{dS_i}{dt} = -\frac{\beta S_i I}{N} \leq 0,$$

so $S_i(t)$ is non-increasing, and $S(t) = \sum S_i(t)$ is non-increasing. Since $S_i(t) > 0$, the limit $S_i(\infty) = \lim_{t\to\infty} S_i(t) \geq 0$ exists, and thus $S(\infty) = \sum S_i(\infty)$ exists. Define $M = \frac{1}{\min\{\gamma_1,\gamma_2,\gamma_3\}}$, so

$$I = \sum I_j \leq M(\gamma_1 I_1 + \gamma_2 I_2 + \gamma_3 I_3).$$

For $R(t) = \sum R_i(t)$,

$$\frac{dS}{dR} = \frac{dS/dt}{dR/dt} = \frac{-\beta S I/N}{(\gamma_1 I_1 + \gamma_2 I_2 + \gamma_3 I_3)} \geq -\frac{\beta M}{N} S.$$

Integrating from $R = 0$ to $R = R(\infty)$,

$$\ln S(\infty) - \ln S(0) \geq -\frac{\beta M}{N} R(\infty).$$

Since $R(t) \leq N$, we have $R(\infty) \leq N$, so

$$S(\infty) \geq S(0) \exp\left(-\frac{\beta M}{N} R(\infty)\right) > 0,$$

as $S(0) > 0$ and $R(\infty) \leq N$.

Part 3: $I(\infty) = 0$**.** Since $\frac{dR_i}{dt} = \gamma_i I_i$ and $R_i(t) \to R_i(\infty) \leq N < \infty$, if $I_i(t)$ does not approach zero, then $\gamma_i I_i$ remains positive, causing $R_i(t) \to \infty$, which contradicts $R_i(t) \leq N$. Thus, $I_i(t) \to 0$, and so $I(t) = \sum I_j(t) \to 0$. □

Lemma 2. *The steady states of system* (2.1) *are characterized by*

$$I_i = 0, \quad S_i + R_i + D_i = N_i, \quad \textit{for all } i = 1, 2, 3,$$

where $S_i, R_i, D_i \geq 0$ *and* N_i *is the total constant population of group i.*

Proof. At the steady state, we set all time derivatives in system (2.1) to zero:

$$\begin{aligned}
\frac{dS_i}{dt} &= -\beta S_i I = 0, \\
\frac{dI_i}{dt} &= \beta S_i I - (\gamma_i + \mu_i) I_i = 0, \\
\frac{dR_i}{dt} &= \gamma_i I_i = 0, \\
\frac{dD_i}{dt} &= \mu_i I_i = 0.
\end{aligned}$$

From the last two equations, we obtain $I_i = 0$. Substituting into the others gives $I = 0$ and thus $\frac{dS_i}{dt} = 0$ is satisfied for any $S_i \geq 0$. Since the model assumes a constant total population $N_i = S_i + I_i + R_i + D_i$, the constraint becomes $S_i + R_i + D_i = N_i$. Therefore, any non-negative values satisfying these constraints define a steady state. □

Theorem 1. *Consider epidemiological model* (2.1) *with a constant total population in each group. Let the disease-free equilibrium (DFE) be given by* $I_i = 0$*,* $R_i = D_i = 0$*, and* $S_i = S_i^* > 0$ *for* $i = 1, 2, 3$*. Then the basic reproduction number* R_0 *is given by*

$$R_0 = \beta \sum_{i=1}^{3} \frac{S_i^*}{\delta_i + \mu_i}. \tag{2.2}$$

Moreover, the DFE is locally asymptotically stable if $R_0 < 1$*, and unstable if* $R_0 > 1$*.*

Proof. To compute R_0, we use the next-generation matrix approach, see, e.g., [8]. Let $x = (I_1, I_2, I_3)^T$ be the vector of infected compartments. The model can be written as:

$$\frac{dx}{dt} = \mathcal{F}(x) - \mathcal{V}(x),$$

where $\mathcal{F}(x)$ is the vector of new infections, and $\mathcal{V}(x)$ is the vector of transitions out of the infected compartments.

At the DFE, where $I_i = 0$ and $S_i = S_i^*$, the Jacobian matrices F, V of $\mathcal{F}$ and $\mathcal{V}$ evaluated at the DFE are:

$$F = \begin{pmatrix} \beta S_1^* & \beta S_1^* & \beta S_1^* \\ \beta S_2^* & \beta S_2^* & \beta S_2^* \\ \beta S_3^* & \beta S_3^* & \beta S_3^* \end{pmatrix}, \quad V = \begin{pmatrix} \delta_1 + \mu_1 & 0 & 0 \\ 0 & \delta_2 + \mu_2 & 0 \\ 0 & 0 & \delta_3 + \mu_3 \end{pmatrix}.$$

The next-generation matrix is given by:

$$K = FV^{-1} = \begin{pmatrix} \frac{\beta S_1^*}{\delta_1+\mu_1} & \frac{\beta S_1^*}{\delta_1+\mu_1} & \frac{\beta S_1^*}{\delta_1+\mu_1} \\ \frac{\beta S_2^*}{\delta_2+\mu_2} & \frac{\beta S_2^*}{\delta_2+\mu_2} & \frac{\beta S_2^*}{\delta_2+\mu_2} \\ \frac{\beta S_3^*}{\delta_3+\mu_3} & \frac{\beta S_3^*}{\delta_3+\mu_3} & \frac{\beta S_3^*}{\delta_3+\mu_3} \end{pmatrix}.$$

This matrix has rank one, and the spectral radius (i.e., the dominant eigenvalue) of K is:

$$R_0 = \rho(K) = \beta \sum_{i=1}^{3} \frac{S_i^*}{\delta_i + \mu_i}.$$

The Jacobian of the infected subsystem at the DFE is $J = F - V$. Since $-V$ is a stable matrix (all eigenvalues have negative real parts), the stability of J is determined by the spectral radius of $K = FV^{-1}$. In particular, if $R_0 = \rho(K) < 1$, then all eigenvalues of J have negative real parts and the DFE is locally asymptotically stable; if $R_0 > 1$, J has a positive eigenvalue and the DFE is unstable. According to the next-generation matrix theory (see [8]), the DFE is locally asymptotically stable if $R_0 < 1$, and unstable if $R_0 > 1$. □

3. Insurance premium calculation

To calculate insurance premiums under epidemic conditions, we integrate the age-stratified epidemic model with actuarial principles. We consider two insurance products: term life insurance (paying a benefit upon death) and critical illness insurance (paying daily benefits for hospitalization upon infection). Premiums are derived using the equivalence principle, equating the expected present value (EPV) of benefits to the EPV of premiums. Insuring infectious disease outbreaks is challenging due to accumulation risk and systemic correlations, but critical illness insurance for infections could be feasible through a public-private partnership (PPP), as proposed by Gründl et al. [27], with government-backed reinsurance to manage high capital requirements. For instance, a policy covering confirmed COVID-19 infections for high-risk groups (e.g., healthcare workers) could be viable, as supported by Harris et al. [24], who found that life insurers maintained stable premiums and offerings for most risk groups during COVID-19, suggesting adaptability to pandemic risks with appropriate risk management.

3.1. State probabilities for individuals

Let $p_S^i(t), p_I^i(t), p_R^i(t), p_D^i(t)$ denote the probabilities that an individual in age group i is susceptible, infected, recovered, or deceased at time t, respectively. For simplicity of notation, we omit the explicit

dependence on time in what follows. These probabilities are defined as normalized proportions of the corresponding compartment sizes in age group i, relative to the initial group size N_i. Recall that N_i is constant. Specifically,

$$p_S^i = \frac{1}{N_i} S_i, p_I^i = \frac{1}{N_i} I_i, p_R^i = \frac{1}{N_i} R_i, p_D^i = \frac{1}{N_i} D_i. \tag{3.1}$$

This interpretation assumes that each individual in age group i is equally likely to be in any of the four disease states, and that the group size N_i remains constant. We define $w_j = \frac{N_j}{N}$ as the initial proportion of the population in age group j, and assume $\sum_{j=1}^{3} w_j = 1$. Then, the total proportion of infectious individuals in the population at time t is given by $\sum_{j=1}^{3} w_j \cdot p_I^j$. It follows from (2.1) that the probability ODEs for age group i are given by

$$\begin{aligned}
\frac{dp_S^i}{dt} &= -\beta \cdot p_S^i \cdot \sum_{j=1}^{3} w_j \cdot p_I^j, \\
\frac{dp_I^i}{dt} &= \beta \cdot p_S^i \cdot \sum_{j=1}^{3} w_j \cdot p_I^j - (\gamma_i + \mu_i) \cdot p_I^i, \\
\frac{dp_R^i}{dt} &= \gamma_i \cdot p_I^i, \\
\frac{dp_D^i}{dt} &= \mu_i \cdot p_I^i.
\end{aligned} \tag{3.2}$$

3.2. Term life insurance premium

The net premium P_{life}^i for a term life insurance policy with benefit 1, term T, and discount rate δ is the expected present value (EPV) of the mortality risk. The premium is:

$$P_{\text{life}}^i = \int_0^T e^{-\delta t} \mu_i p_I^i(t)\, dt, \tag{3.3}$$

where:

- μ_i: Mortality rate for age group i.
- $p_I^i(t)$: Probability of being in the infectious state at time t.
- $e^{-\delta t}$: Discount factor, with δ as the force of interest.
- T: Policy term.

While standard actuarial models include explicit survival probabilities, here $p_I^i(t)$ naturally incorporates survival through state transitions in the epidemic model, so no additional survival term is needed.

Lemma 3. *Under constant prevalence $I(t) \equiv I_0$, the term life insurance premium for age group i, with benefit 1, term T, and discount rate δ, is:*

$$P_{life}^i = \mu_i \cdot \frac{\beta \frac{I_0}{N}}{\gamma_i + \mu_i - \beta \frac{I_0}{N}} \left[\frac{1 - e^{-(\delta + \beta \frac{I_0}{N})T}}{\delta + \beta \frac{I_0}{N}} - \frac{1 - e^{-(\delta + \gamma_i + \mu_i)T}}{\delta + \gamma_i + \mu_i} \right],$$

assuming $\beta \frac{I_0}{N} \neq \gamma_i + \mu_i$.

Proof. With $I(t) \equiv I_0$, it follows from (3.2) that the ODE for susceptibles is

$$\frac{dp_S^i}{dt} = -\beta \frac{I_0}{N} p_S^i, \quad p_S^i(0) = 1,$$

whose solution is

$$p_S^i(t) = e^{-\beta \frac{I_0}{N} t}.$$

The infected compartment satisfies

$$\frac{dp_I^i}{dt} = \beta \frac{I_0}{N} p_S^i - (\gamma_i + \mu_i) p_I^i, \quad p_I^i(0) = 0.$$

Using an integrating factor $e^{(\gamma_i+\mu_i)t}$, the solution is

$$p_I^i(t) = \frac{\beta \frac{I_0}{N}}{(\gamma_i + \mu_i) - \beta \frac{I_0}{N}} \left(e^{-\beta \frac{I_0}{N} t} - e^{-(\gamma_i+\mu_i)t} \right).$$

The premium integral is

$$\begin{aligned} P^i_{\text{life}} &= \mu_i \cdot \frac{\beta \frac{I_0}{N}}{\gamma_i + \mu_i - \beta \frac{I_0}{N}} \int_0^T e^{-\delta t} \left[e^{-\beta \frac{I_0}{N} t} - e^{-(\gamma_i+\mu_i)t} \right] dt \\ &= \mu_i \cdot \frac{\beta \frac{I_0}{N}}{\gamma_i + \mu_i - \beta \frac{I_0}{N}} \left[\frac{1 - e^{-(\delta + \beta \frac{I_0}{N})T}}{\delta + \beta \frac{I_0}{N}} - \frac{1 - e^{-(\delta+\gamma_i+\mu_i)T}}{\delta + \gamma_i + \mu_i} \right]. \end{aligned}$$

□

We note that, a priori, it is not clear why the expression in the lemma is non-negative. However, since it is obtained as an integral involving p_I^i in (3.3), and the non-negativity of p_I^i follows directly from its definition and Lemma 1, the result is immediate.

3.3. Health insurance premium

The health insurance premium P^i_{hospital} pays a daily benefit c_h during hospitalization (infectious state) over term $[0, T]$. The expected cost of hospitalization for an individual in age group i is the EPV of payments made while hospitalized. The premium is:

$$P^i_{\text{hospital}} = c_h \int_0^T e^{-\delta t} p_I^i(t)\, dt,$$

where:

- c_h: Daily hospitalization cost (e.g., dollars per day).
- $p_I^i(t)$: Probability of being in the infectious (hospitalized) state at time t.
- $e^{-\delta t}$: Discount factor, with δ as the force of interest.
- T: Policy term (in days).

This formula integrates the expected time spent in the hospitalized state, weighted by the daily cost and discounted to the present value. Under constant prevalence, the formula simplifies as shown in Lemma 3. The following lemma presents the simplified expression. The proof is analogous and is therefore omitted.

Lemma 4. *Under constant prevalence $I(t) \equiv I_0$, the health insurance premium for age group i, with daily hospitalization cost c_h, term T, and discount rate δ, is:*

$$P^i_{hospital} = c_h \cdot \frac{\beta\frac{I_0}{N}}{\gamma_i + \mu_i - \beta\frac{I_0}{N}} \left[\frac{1 - e^{-(\delta+\beta\frac{I_0}{N})T}}{\delta + \beta\frac{I_0}{N}} - \frac{1 - e^{-(\delta+\gamma_i+\mu_i)T}}{\delta + \gamma_i + \mu_i} \right],$$

assuming $\beta\frac{I_0}{N} \neq \gamma_i + \mu_i$.

3.4. Reserve calculations

In actuarial science, a reserve is the amount an insurer must hold to meet future obligations under an insurance contract, calculated as the expected present value of future benefits less future premiums [28]. The prospective reserve at time t for a term life insurance policy issued at time 0 for age group i, with benefit 1 and term T, is the EPV of future benefits, assuming a single premium was paid at inception. The reserve is:

$$V^i_{\text{life}}(t) = \int_t^T e^{-\delta(\tau-t)} \mu_i p^i_I(\tau)\, d\tau,$$

where:

- μ_i: Mortality rate for age group i.
- $p^i_I(\tau)$: Probability of being in the infectious state at time τ.
- $e^{-\delta(\tau-t)}$: Discount factor, with δ as the force of interest.
- T: Policy term.

While standard actuarial models include explicit survival probabilities, here p^i_I incorporates survival through state transitions in the epidemic model, requiring no additional term. The reserve requires ongoing updates to p^i_I based on the evolving epidemic.

4. Modeling recovery and death

To simplify the modeling process, several assumptions are made regarding the age-dependent parameters. Empirical findings (see, e.g., [29]) suggest that the recovery period is positively correlated with age. This is supported by data-driven analyses of COVID-19 in the province of Pavia, Italy, where Zanella et al. [30, 31] used detailed health agency data to quantify age-dependent recovery dynamics and social contact patterns. Their findings indicate that older individuals exhibit longer recovery times, consistent with the proposed inverse relationship, and highlight the role of social contact heterogeneity in shaping epidemic spread, informing our model's parameterization. Therefore, since the recovery rate is the inverse of the recovery period, it can be modeled as

$$\gamma(a) = \frac{1}{k + ma}, \tag{4.1}$$

where k and m are positive constants. This reflects the understanding that older individuals generally recover more slowly from infectious diseases due to age-related declines in physiological resilience.

As for the disease-induced mortality rate $\mu(a)$, from [32], we observe that the age-specific mortality rate shows an exponential growth rate [32]. Hence, we assume

$$\mu(a) = ce^{da}, \tag{4.2}$$

where c and d are positive constants.

We divide the population into three age groups, separated by ages $0 = a_0 < a_1 < a_2 < a_3 = 100$. Aside from parameter estimation, our goal is to determine a_1 and a_2, subject to the constraints $20 \leq a_1 \leq 30$ and $50 \leq a_2 \leq 70$. Let $p(a)$ denote the population age distribution, normalized such that $\int_0^{100} p(a)\,da = 1$. The fraction of the population in age group i (for $i = 1, 2, 3$) is given by

$$P_i = \int_{a_{i-1}}^{a_i} p(a)\,da. \tag{4.3}$$

The recovery rate γ_i for age group i is defined as the population-weighted average of $\gamma(a)$ over the interval $[a_{i-1}, a_i]$:

$$\gamma_i = \frac{1}{P_i}\int_{a_{i-1}}^{a_i} \gamma(a)p(a)\,da = \frac{1}{P_i}\int_{a_{i-1}}^{a_i} \frac{p(a)}{k+ma}\,da. \tag{4.4}$$

Similarly, the mortality rate μ_i for age group i is defined as:

$$\mu_i = \frac{1}{P_i}\int_{a_{i-1}}^{a_i} \mu(a)p(a)\,da = \frac{1}{P_i}\int_{a_{i-1}}^{a_i} ce^{da}p(a)\,da. \tag{4.5}$$

4.1. Simplified formulas under uniform population density

In the absence of specific population age distribution data, one may assume a uniform population density over $[0, 100]$, i.e., $p(a) = \frac{1}{100}$. Under this assumption, the population-weighted averages for γ_i and μ_i simplify to the unweighted averages over the age intervals.

Lemma 5. *If the population age distribution is uniform, i.e., $p(a) = \frac{1}{100}$ for $a \in [0, 100]$, then the recovery and mortality rates for age group i are:*

$$\gamma_i = \frac{1}{a_i - a_{i-1}}\int_{a_{i-1}}^{a_i} \frac{1}{k+ma}\,da = \frac{1}{(a_i - a_{i-1})m}\ln\left(\frac{k+ma_i}{k+ma_{i-1}}\right), \tag{4.6}$$

$$\mu_i = \frac{1}{a_i - a_{i-1}}\int_{a_{i-1}}^{a_i} ce^{da}\,da = \frac{c}{(a_i - a_{i-1})d}\left[e^{da_i} - e^{da_{i-1}}\right]. \tag{4.7}$$

5. Numerical parameter estimation and premium-reserve analysis

To estimate the parameters β, k, m, c, d, a_1, and a_2, we aim to minimize the difference between model-predicted confirmed cases and observed data in the age-structured SIRD model defined in Section 2. For this analysis, we use COVID-19 data from Uzbekistan during the first 31 days of the outbreak [33]. The first confirmed case in Uzbekistan was reported on March 15, 2020. Let $\hat{C}_i(t_k)$ denote the model-predicted number of confirmed cases in age group i at time t_k (for $k = 1, 2, \ldots, K$,

where t_1 corresponds to March 15, 2020), and let $C_i(t_k)$ represent the observed confirmed cases. The population age distribution for Uzbekistan, shown in Figure 2, is taken from [34]. The incidence of new infections in group i at time t is given by $\frac{\beta S_i(t)I(t)}{N}$. Hence, the confirmed cases over a time interval $[t_k, t_{k+1}]$ are:

$$\hat{C}_i(t_k) = \int_{t_k}^{t_{k+1}} \frac{\beta S_i(t)I(t)}{N}\, dt. \tag{5.1}$$

The objective function is the sum of squared errors between predicted and observed confirmed cases:

$$J(\beta, k, m, c, d, a_1, a_2) = \sum_{k=1}^{K} \sum_{i=1}^{3} \left[\hat{C}_i(t_k) - C_i(t_k)\right]^2, \tag{5.2}$$

subject to the constraints $k > 0$, $m > 0$, $c > 0$, $d > 0$, $20 \le a_1 \le 30$, and $50 \le a_2 \le 70$. If age-specific case data is unavailable, the total confirmed cases across all groups, $C_{\text{total}}(t_k) = \sum_{i=1}^{3} C_i(t_k)$, can be used, with the objective function:

$$J(\beta, k, m, c, d, a_1, a_2) = \frac{1}{K} \sum_{k=1}^{K} \left[\hat{C}_{\text{total}}(t_k) - C_{\text{total}}(t_k)\right]^2. \tag{5.3}$$

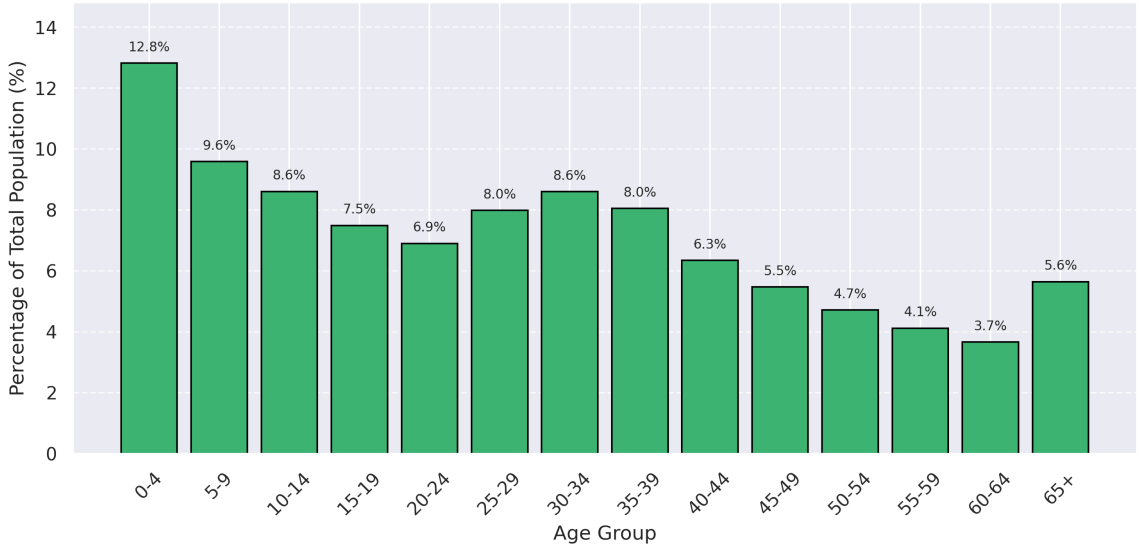

Figure 2. Population distribution by age group in Uzbekistan (July 1, 2024).

To solve the optimization problem in Eq (5.3), we employ a genetic algorithm (GA), a stochastic, population-based search method inspired by natural selection. The GA begins with a randomly initialized population of 20 individuals, each representing a candidate parameter vector sampled within predefined bounds: $\beta \in [0.1, 2.0]$, $k \in [1.0, 10.0]$, $m \in [0.001, 0.3]$, $c \in [10^{-6}, 10^{-3}]$, $d \in [0.001, 0.03]$, $a_1 \in [20.0, 30.0]$, and $a_2 \in [50.0, 70.0]$. The algorithm proceeds for up to 20 generations, using tournament selection (size 3), blend crossover (probability $c_{\text{xp}} = 0.7$), and Gaussian mutation (probability $p_{\text{mut}} = 0.2$) with bounds enforcement. At each generation, individuals are evaluated by solving the age-structured SIRD model using `odeint`, computing the predicted

cumulative incidence, and minimizing the objective function. The parameter set that yields the lowest error is selected as the optimal estimate.

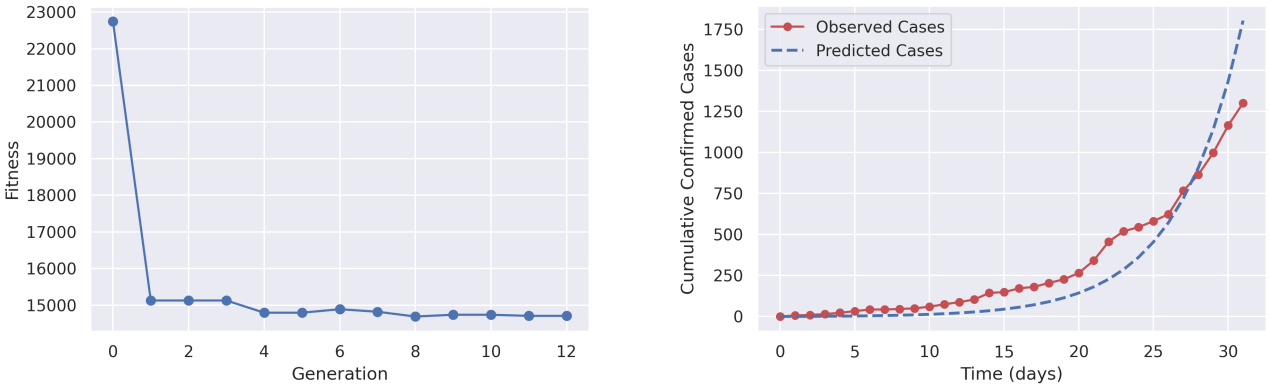

(a) Best Fitness per Generation

(b) Predicted vs. Observed COVID-19 Cases

Figure 3. (a) Fitness evolution over generations. (b) Model prediction compared to observed COVID-19 data.

The GA converged in 13 generations, after which early stopping was triggered due to negligible improvement in the objective function over five successive generations (less than 0.1%). Table 1 summarizes the final optimized parameters that minimize the objective function defined in Eq (5.3). The optimal parameter values yielded a mean squared error of 14,708.34 between the model predictions and the observed confirmed cases. Using (2.2) we estimate the basic reproduction number $R_0 = 4.458$. Figure 3 illustrates the optimization process. Figure 3(a) shows the progression of the best objective function value across generations, indicating rapid convergence within the first few iterations. Figure 3(b) compares the predicted cumulative confirmed cases from the age-structured SIRD model using the optimized parameters with the observed data, demonstrating a strong fit.

Table 1. Final optimized parameters and derived rates.

Optimized Parameters			**Derived Rates**		
Parameter	**Description**	**Value**	**Parameter**	**Description**	**Value**
β	Transmission rate	0.3063	γ_1	Recovery rate (age group 1)	0.1152
k	Gamma shape (recovery)	6.4163	γ_2	Recovery rate (age group 2)	0.0568
m	Gamma scale (recovery)	0.3013	γ_3	Recovery rate (age group 3)	0.0315
c	Gamma shape (mortality)	0.000429	μ_1	Mortality rate (age group 1)	0.00052
d	Gamma scale (mortality)	0.0210	μ_2	Mortality rate (age group 2)	0.00102
a_1	First age threshold	20.52	μ_3	Mortality rate (age group 3)	0.00260
a_2	Second age threshold	69.89	R_0	Basic reproduction number	4.458

Figure 4 presents the simulated epidemic dynamics over a one-year horizon using the age-structured SIRD model parameterized by the optimized values. The figure illustrates the temporal evolution of susceptible, infected, recovered, and deceased populations, capturing the characteristic progression and eventual stabilization of the outbreak under the estimated parameters.

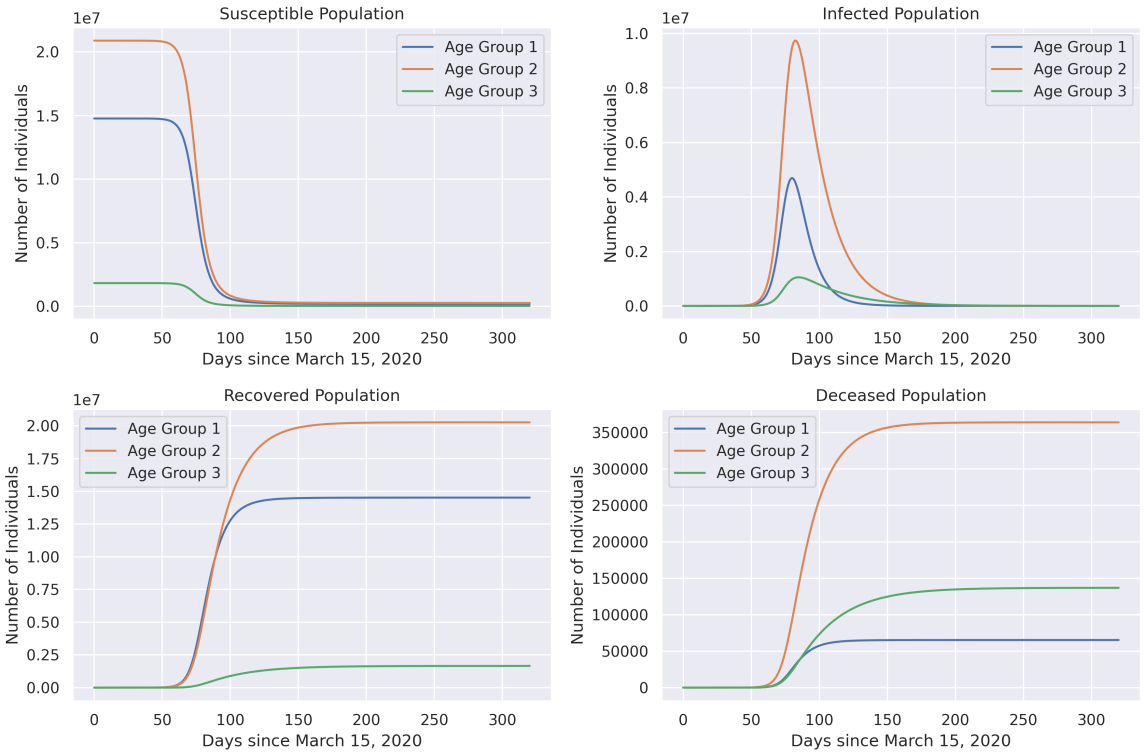

Figure 4. Simulated SIRD dynamics for one year.

Table 2. Life insurance premiums by age group (Benefit = 1, $T = 365$, $\delta = 0.05/365$).

Age Group	Premium
0–20	4.37902×10^{-3}
20–70	1.72176×10^{-2}
70–100	7.43063×10^{-2}

Table 2 displays the life insurance premiums for a one-year term ($T = 365$) across age groups 0–20, 20–70, and 70–100, calculated with a benefit of 1 and a daily discount rate $\delta = 0.05/365$. Using the optimized parameters from Table 1, the premiums reflect the expected present value of benefits based on mortality rates μ_i and infectious state probabilities p_I^i from the age-structured SIRD model. The 70–100 age group incurs the highest premium, driven by its elevated mortality risk.

Table 3. Health insurance premiums by age group for months 1–6 (Benefit = 1, $\delta = 0.05/365$).

Age Group	Month 1	Month 2	Month 3	Month 4	Month 5	Month 6
0–20	0.00017	0.17248	6.56175	8.34249	8.46989	8.48510
20–70	0.00020	0.20815	9.86132	15.67456	16.89701	17.14216
70–100	0.00022	0.22859	12.23692	23.41061	28.00537	29.82116

Table 3 presents the health insurance premiums for age groups 0–20, 20–70, and 70–100 over the first six months (30, 60, 90, 120, 150, and 180 days), calculated using the optimized parameters from

Table 1 with a daily discount rate $\delta = 0.05/365$ and a benefit of 1. These premiums, derived from the age-structured SIRD model's infectious state probabilities p_I^i, show a marked increase with age and policy duration, with the 70–100 age group facing the highest costs due to higher susceptibility and slower recovery. Figure 5 illustrates the prospective life insurance reserves over a one-year term ($T = 365$), computed using the mortality rates μ_i and p_I^i from the same model. The reserves, reflecting the expected present value of future benefits, exhibit distinct trajectories across age groups, with the 70–100 group showing the steepest reserve requirements due to elevated mortality risks.

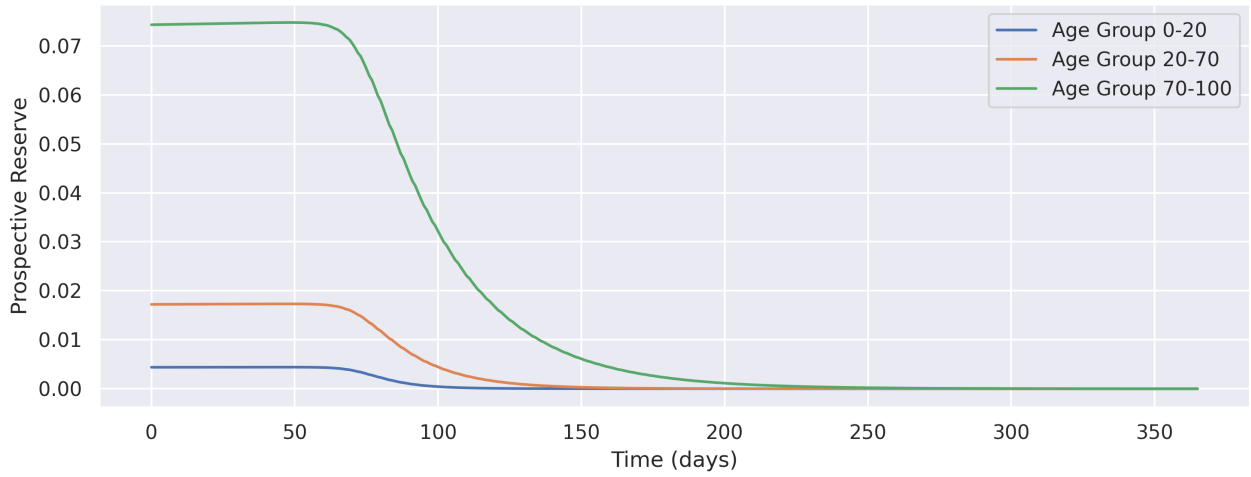

Figure 5. Life insurance reserves over time.

6. Sensitivity of life insurance premiums to the estimated parameters

In this section, we provide the sensitivity analysis by employing a global sensitivity framework. To assess the robustness of our age-stratified compartmental model and its implications for life insurance premium calculations, we conduct a *global sensitivity analysis* using the partial rank correlation coefficient (PRCC) method. Specifically, we generate 2000 Latin hypercube samples of key model parameters, namely β, k, m, c, d, a_1, and a_2, within a range of $\pm 10\%$ of their baseline values. These parameters govern the age-specific recovery rate $\gamma(a) = 1/(k + ma)$, mortality rate $\mu(a) = ce^{da}$, and the age cutoffs a_1 and a_2 that define the age groups under consideration.

For each sample, we compute the life insurance premium for the given age group by solving the age-structured ODE system and discounting future mortality benefits. The true PRCC coefficients are then computed by first ranking both the inputs and output, removing the effects of other variables through multivariate regression, and then measuring Pearson's correlation of the residuals. This procedure quantifies the strength and direction of the monotonic relationship between each parameter and the premium while controlling for all other parameters. To perform this analysis, we employ Latin hypercube sampling and the true PRCC, following the approach of [35], who used the PRCC to assess the sensitivity of the basic reproduction number R_0 and mortality outcomes to vaccination strategies in an epidemic model. The true PRCC method is particularly appropriate for our age-structured, nonlinearly coupled system, where we aim to control for multivariate effects. Our procedure is analogous to methods previously described in [7].

To visualize and compare how different model parameters influence the life insurance premium across age groups, we present in Figure 6 a grouped bar chart of the true PRCC for each age group. This graphical representation reveals both similarities and differences in parameter sensitivities across age groups. Certain parameters, such as the recovery rate constant k and mortality scaling d, exhibit consistently strong correlations across all groups, reflecting their universal influence on the pricing structure. Specifically, the recovery parameter k shows a large, positively strong PRCC across age groups, suggesting its robust impact on premium estimates.

Other parameters, however, demonstrate age-specific effects. For example, the parameter a_1, which defines the boundary between the youngest and middle age groups, shows a strong and positive association with the premium in the first group but weakens or reverses in the subsequent groups. Furthermore, a_2, marking the division between middle and elderly groups, displays a greater influence in the elderly subgroup, reflecting the growing role of age-related mortality and recovery in pricing policy.

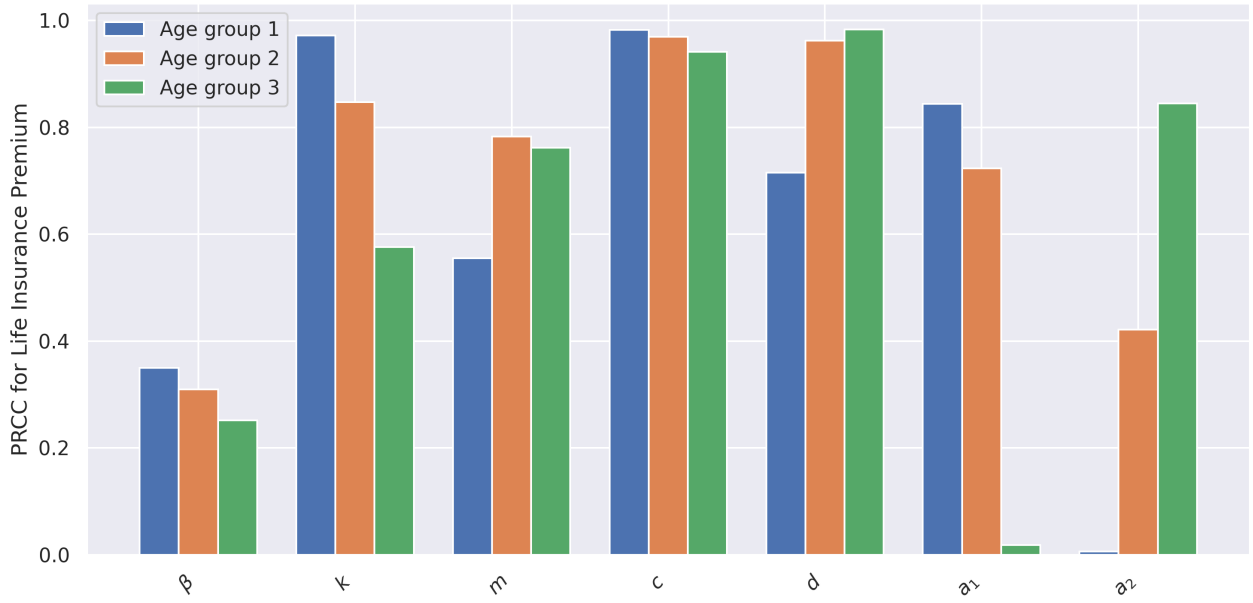

Figure 6. Comparison of the PRCC of life insurance premiums across age groups.

7. Discussion and conclusions

This study presents a novel integration of age-stratified epidemic modeling and actuarial science to address insurance pricing challenges during pandemics. Our compartmental age-structured SIRD model, calibrated with genetic algorithms and real-world COVID-19 data, underscores the critical role of age-specific recovery and mortality rates in shaping premiums and reserves. Premiums for the elderly (age 70+) are significantly higher, nearly 17 times higher than for younger groups, reflecting elevated mortality risks. Reserve trajectories show non-monotonic patterns, peaking during epidemic surges and stabilizing as infections decline. Sensitivity analysis highlights that the recovery rate constant k and mortality scaling d strongly influence premium estimates, emphasizing the need for precise parameter calibration. However, model predictions, such as those in Figure 3(b), may be

sensitive to hyperparameters like the time horizon used for estimation. A shorter time horizon could enhance accuracy, though optimal settings for real-life insurance applications remain uncertain, suggesting a need for alternative models or estimation methods. The model's reliance on uniform mixing and static contact patterns limits its applicability in heterogeneous settings, necessitating further refinements.

Our proposed recovery rate $\gamma(a) = 1/(k + ma)$ (Eq (4.1)) is deliberately simple, analytically tractable, and consistent with empirical findings that recovery time increases with age [29]. This form facilitates closed-form derivations and transparent sensitivity analysis in the actuarial context. At the same time, more general data-driven recovery functions have been explored in the literature. For example, Zanella et al. [30] fitted a piecewise-exponential $\gamma(a)$ to Italian COVID-19 data, while Albi et al. [36] employed a flat-then-exponential structure. These richer forms capture finer age-specific heterogeneity and improve epidemic fit, though at the cost of additional complexity. Hence, our formulation should be viewed as a parsimonious baseline for actuarial applications, complementary to more detailed epidemiological specifications.

Non-pharmaceutical interventions (NPIs), such as social distancing or mask mandates, can reduce transmission rates, lowering infection probabilities and thus insurance premiums and reserves. However, NPIs impose economic and social costs, creating a trade-off between reduced insurer liabilities and broader macroeconomic impacts on policyholder affordability. The framework remains flexible for future epidemics through updated parameters but could be enhanced by incorporating behavioral responses, vaccination effects, or NPI-driven changes in transmission dynamics. Exploring varied hyperparameter configurations, such as time horizons, genetic algorithm settings, or numerical integration step sizes, could further improve model performance for practical insurance pricing. Overall, this approach offers insurers a data-informed tool for solvency management during health crises, balancing risk mitigation with affordability.

Use of AI tools declaration

The authors declare they have not used Artificial Intelligence (AI) tools in the creation of this article.

Acknowledgments

The first author acknowledges the support of a grant from the Ministry of Science and Higher Education of the Republic of Kazakhstan within the framework of the project AP19676669.

Conflict of interest

The authors declare there is no conflict of interest.

References

1. L. Francis, M. Steffensen, Epidemiological modeling in life insurance, *Soc. Sci. Res. Network*, **28** (2022), 1–28. https://doi.org/10.2139/ssrn.4238013
2. G. Di Lorenzo, G. Franchetti, M. Politano, A premium structure for a pandemic insurance policy, *Electron. J. Appl. Stat. Anal.*, **17** (2024), 703–734. https://doi.org/10.1285/i20705948v17n3p703

3. L. Francis, M. Steffensen, Individual life insurance during epidemics, *Ann. Actuar. Sci.*, **18** (2024), 152–175. https://doi.org/10.1017/S1748499523000209
4. C. Zhai, P. Chen, Z. Jin, T. K. Siu, Epidemic modelling and actuarial applications for pandemic insurance: A case study of Victoria, Australia, *Ann. Actuar. Sci.*, **18** (2024), 242–269. https://doi.org/10.1017/S1748499523000246
5. R. F. Arthur, M. Levin, A. Labrogere, M. W. Feldman, Age classes stratified by risk and adaptive behavior during epidemics, preprint, arXiv:2023.05.30.23290737. https://doi.org/10.1101/2023.05.30.23290737
6. N. G. Davies, P. Klepac, Y. Liu, K. Prem, M. Jit, R. M. Eggo, et al., Age-dependent effects in the transmission and control of COVID-19 epidemics, *Nat. Med.*, **26** (2020), 1205–1211. https://doi.org/10.1038/s41591-020-0962-9
7. K. Kim, J. W. Choi, J. Moon, H. Akilov, L. Tuychiev, B. Rakhimov, et al., Clinical features of COVID-19 in Uzbekistan, *J. Korean Med. Sci.*, **35** (2020), e404. https://doi.org/10.3346/jkms.2020.35.e404
8. P. Driessche, J. Watmough, Reproduction numbers and sub-threshold endemic equilibria for compartmental models of disease transmission, *Math. Biosci.*, **180** (2002), 29–48. https://doi.org/10.1016/S0025-5564(02)00108-6
9. Y. Amemiya, T. Li, H. Nishiura, Age-dependent final size equation to anticipate mortality impact of COVID-19 in China, *Math. Biosci. Eng.*, **20** (2023), 11353–11366. https://doi.org/10.3934/mbe.2023503
10. Q. Yan, X. Liu, Dynamics of an epidemic model with general incidence rate dependent on a class of disease-related contact functions, *Math. Biosci. Eng.*, **20** (2023), 20795–20808. https://doi.org/10.3934/mbe.2023920
11. M. De la Sen, A. Ibeas, S. Alonso-Quesada, R. Nistal, On a new epidemic model with asymptomatic and dead-infective subpopulations with feedback controls useful for Ebola disease, *Discrete Dyn. Nat. Soc.*, **2017** (2017), 4232971. https://doi.org/10.1155/2017/4232971
12. N. H. Shah, Z. A. Patel, B. M. Yeolekar, Vertical dynamics of Ebola with media impact, *J. King Saud Univ. Sci.*, **31** (2019), 567–574. https://doi.org/10.1016/j.jksus.2018.03.011
13. Q. Niu, H. Li, Y. Liu, Z. Qin, L. Zhang, J. Chen, Z. Lyu, Toward the Internet of medical things: Architecture, trends and challenges, *Math. Biosci. Eng.*, **21** (2024), 650–678. https://doi.org/10.3934/mbe.2024028
14. Y. Ye, Q. Zhang, X. Wei, Z. Cao, H. Y. Yuan, D. D. Zeng, Equitable access to COVID-19 vaccines makes a life-saving difference to all countries, *Nat. Hum. Behav.*, **6** (2022), 207–216. https://doi.org/10.1038/s41562-022-01289-8
15. C. C. Zhu, J. Zhu, X. L. Liu, Influence of spatial heterogeneous environment on long-term dynamics of a reaction-diffusion SVIR epidemic model with relapse, *Math. Biosci. Eng.*, **16** (2019), 5897–5922. https://doi.org/10.3934/mbe.2019295
16. C. C. Pacheco, C. R. de Lacerda, Function estimation and regularization in the SIRD model applied to the COVID-19 pandemics, *Inverse Probl. Sci. Eng.*, **29** (2021), 1613–1628. https://doi.org/10.1080/17415977.2021.1872563

17. Z. Yin, Y. Yu, Z. Lu, Stability analysis of an age-structured SEIRS model with time delay, *Mathematics*, **8** (2020), 455. https://doi.org/10.3390/math8030455

18. C. Cakmakli, Y. Simsek, Bridging the COVID-19 data and the epidemiological model using the time-varying parameter SIRD model, *J. Econom.*, **242** (2024), 105787. https://doi.org/10.1016/j.jeconom.2024.105787

19. O. N. Oyelade, A. E. S. Ezugwu, T. I. A. Mohamed, L. Abualigah, Ebola optimization search algorithm: A new nature-inspired metaheuristic optimization algorithm, *IEEE Access*, **10** (2022), 16150–16177. https://doi.org/10.1109/ACCESS.2022.3147821

20. R. El Chaal, S. Bouchefra, M. O. Aboutafail, Stochastic dynamics and extinction time in SIR epidemiological models, *Acadlore Trans. Appl. Math. Stat.*, **1** (2023), 181–202. https://doi.org/10.56578/atams010305

21. S. Cox, J. Fairchild, H. Pedersen, Valuation of structured risk management products, *Insur. Math. Econ.*, **34** (2004), 259–272. https://doi.org/10.1016/j.insmatheco.2003.12.006

22. R. Feng, J. Garrido, L. Jin, S. H. Loke, L. Zhang, Epidemic compartmental models and their insurance applications, in *Pandemics: Insurance and Social Protection*, Springer, **2** (2022), 13–40. https://doi.org/10.1007/978-3-030-78334-1_2

23. E. Guerra, *An Application of Deterministic Epidemic Models to the Calculation of Insurance Premiums and Benefit Reserve Values*, Master's thesis, California State Polytechnic University, 2022.

24. T. F. Harris, A. Yelowitz, C. Courtemanche, Did COVID-19 change life insurance offerings?, *J. Risk Insur.*, **88** (2021), 831–861. https://doi.org/10.1111/jori.12344

25. L. Ferretti, C. Wymant, M. Kendall, L. Zhao, A. Nurtay, L. Abeler-Dörner, et al., Quantifying SARS-CoV-2 transmission suggests epidemic control with digital contact tracing, *Science*, **368** (2020), eabb6936. https://doi.org/10.1126/science.abb6936

26. P. Manfredi, A. D'Onofrio, *Modeling the Interplay between Human Behavior and the Spread of Infectious Diseases*, Springer, New York, 2013. https://doi.org/10.1007/978-1-4614-5474-8

27. H. Gründl, D. Guxha, A. Kartasheva, H. Schmeiser, Insurability of pandemic risks, *J. Risk Insur.*, **88** (2021), 863–902. https://doi.org/10.1111/jori.12368

28. D. C. M. Dickson, M. R. Hardy, H. R. Waters, *Actuarial Mathematics for Life Contingent Risks*, 2nd edition, Cambridge University Press, Cambridge, 2020.

29. I. Voinsky, G. Baristaite, D. Gurwitz, Effects of age and sex on recovery from COVID-19: Analysis of 5769 Israeli patients, *J. Infect.*, **81** (2020), e102–e103. https://doi.org/10.1016/j.jinf.2020.05.026

30. M. Zanella, C. Bardelli, M. Azzi, S. Deandrea, P. Perotti, S. Silva, et al., Social contacts, epidemic spreading and health system. Mathematical modeling and applications to COVID-19 infection, *Math. Biosci. Eng.*, **18** (2021), 3384–3403. https://doi.org/10.3934/mbe.2021169

31. M. Zanella, C. Bardelli, G. Dimarco, S. Deandrea, P. Perotti, M. Azzi, et al., A data-driven epidemic model with social structure for understanding the COVID-19 infection on a heavily affected Italian Province, *Math. Models Methods Appl. Sci.*, **31** (2021), 2533–2570. https://doi.org/10.1142/S021820252150055X

32. J. R. Goldstein, R. D. Lee, Demographic perspectives on the mortality of COVID-19 and other epidemics, *Proc. Natl. Acad. Sci. USA*, **117** (2020), 22035–22041. https://doi.org/10.1073/pnas.2006392117

33. Johns Hopkins University CSSE, *2019 Novel Coronavirus COVID-19 Data Repository*, 2020. Available from: https://github.com/CSSEGISandData/COVID-19.

34. Statistics Agency under the President of the Republic of Uzbekistan, Demographic situation in the Republic of Uzbekistan (press release), 2024. Available from: https://stat.uz/img/demografiya-press-reliz-22_07_2024-english-_p27562.pdf.

35. D. Bolatova, S. Kadyrov, A. Kashkynbayev, Mathematical modeling of infectious diseases and the impact of vaccination strategies, *Math. Biosci. Eng.*, **21** (2024), 7103–7123. https://doi.org/10.3934/mbe.2024314

36. G. Albi, L. Pareschi, M. Zanella, Control with uncertain data of socially structured compartmental epidemic models, *J. Math. Biol.*, **82** (2021), 63. https://doi.org/10.1007/s00285-021-01617-y

AIMS Press